-RESEARCH PAPER-

International Journal of Mining and Geo-Engineering

IJMGE

IJMGE 58-3 (2024) 263-270

DOI: 10.22059/IJMGE.2024.370406.595136

Geophysical simulation of landslide model based on electrical resistivity and refraction seismic tomography through unstructured meshing

Amir Yazdanpanah [a], Maysam Abedi [a, *]

[a] *School of Mining Engineering, College of Engineering, University of Tehran, Tehran, Iran.*

Article History:

Received: 31 December 2023.
Revised: 15 January 2024.
Accepted: 12 February 2024.

ABSTRACT

Mass movements of land, such as landslides, pose significant threats to human safety and infrastructure. This study focuses on advancing the understanding of landslide dynamics through the application of geophysical surveys, specifically the Electrical Resistivity Tomography (ERT) and Seismic Refraction Tomography (SRT). Unstructured meshing, as a pivotal technique in geophysics simulation studies, provides flexibility in discretizing complex geological structures. This method allows for refined mesh elements where needed, optimizing computational resources. In the field of geophysics, unstructured meshing is particularly advantageous for accurately representing subsurface heterogeneities. This study employs pyGIMLi, a Geophysical Inversion and Modelling Python library. This Python programming library, although devoid of a GUI, offers a comprehensive suite of tools for geophysical data analysis and inversion. This library incorporates unstructured meshing capabilities. This feature enhances the accuracy of simulations, enabling researchers to model intricate geological formations with more precision. Using this library empowers users to seamlessly generate, manipulate, and analyze unstructured meshes, facilitating robust simulations and detailed investigations of subsurface properties in geophysics. In this study, we present a novel approach to simulate a three-layered landslide using the ERT and SRT, coupled with inverse modelling through utilizing the unstructured meshing of the inversion area. The synthetic model produced has a depth of study extending to 65 meters. The SRT model reveals a dense coverage in layer 2, providing crucial information about the subsurface characteristics. The utilization of the ERT and SRT in tandem allows for a comprehensive understanding of the landslide structure, offering insights into detecting the slip surface of the landslide. The study's innovative methodology provides a robust framework for the analysis of complex geological scenarios. The results obtained from this simulation contribute to the broader knowledge of landslide dynamics and offer a valuable tool for assessing and mitigating landslide risks in similar geological settings.

Keywords: *Landslide, ERT, SRT, pyGIMLi, Unstructured meshing.*

1. Introduction

Geohazard phenomena have the potential to harm or heighten the vulnerability of humans, assets, vital infrastructure, and the surrounding environment. These events may lead to the disruption of human endeavors, resulting in significant socioeconomic implications. Among various natural incidents, landslides are recognized as particularly destructive geohazards (Fig.1). Landslides fall under the category of "mass wasting," indicating the downward displacement of soil and rock influenced directly by gravity. Such incidents can manifest in diverse sizes and forms [1]. Landslides present intricate formations with diverse geological, geomorphological, and hydrogeological characteristics. Exploring these heterogeneous structures poses a significant challenge for near-surface geophysics. The advancement of both 2D and 3D geophysical methods has sparked increasing enthusiasm for evaluating landslide volume, delineating the physical attributes of the landslide material, and identifying groundwater movements within and surrounding the slide. In these varied structures, employing a combination of diverse geophysical methods has proven essential for achieving dependable outcomes. The selection of techniques is evidently influenced by the anticipated differences in physical parameters [2].

In the case of the use of geophysical methods in landslide studies, in 2020, Whiteley put forth an elementary technique and systematic procedure to generate a dependable sequence of seismic velocity models through inversion over time [3]. In 2012, Carpentier collected data from trenches, GPS, electrical resistivity tomography, and Ground-Penetrating Radar (GPR), unveiling detailed images depicting the composition and structure of historical and potential future landslides [4]. In 2021, Imani stated that the seismic refraction tomography method is proficient in delineating the slope material, the geometry of the sliding surface, the dynamics of landslide mass movement, the physical properties of the terrain, and the impact of water saturation on the slope [5]. In 2018, Pappalardo studied a landslide by conducting passive seismic surveys. Employing these surveys through ambient noise acquisition, facilitated the identification of impedance contrasts, particularly linked to distinctive features, such as the landslide body. These findings were subsequently supported by the results obtained from an electrical resistivity survey [6].

In 2021, Whitely used three geophysical methods in order to study a landslide in the UK. Firstly, the topography data were collected by an Unmanned Aerial Vehicle (UAV) survey. Consequently, the heterogeneity of the landslide was studied using the unsupervised classification of electrical resistivity and seismic refraction surveys [7]. In 2019, Rezaei utilized the electrical resistivity tomography 2D imaging

* Corresponding author. *E-mail address:* maysamabedi@ut.ac.ir (M. Abedi).

in order to detect a landslide surface [8]. In 2021, Zainal used the SRT to explore the structural layout of the sliding area in the aftermath of a landslide incident in Indonesia [9]. In 2021, Rehman used both GPR and ERT as two non-invasive geophysical methods to asses a landslide subsurface [10]. In 2023, Yang employed elastic full waveform inversion to detect a landslide area in Peru [11]. In 2022, Damavandi studied a landslide slip surface by the ERT survey. The model is derived through an inversion using both structured and unstructured meshing [12]. In 2019, Chen utilized an integration of ERT, SRT, and Seismic Scattered wave Imaging (SSI) to evaluate a landslide area [13]. In 2019, Pasierb detected a landslide slip surface using the ERT and geotechnical assessments, such as Cone Penetration Test (CPTU) and drilling [14]. In 2022, Himi obtained a 3D geological model of a landslide body utilizing ERT, SRT, and borehole data [15]. In 2019, Huntley investigated a very slow-moving landslide by employing a multi-technique geophysical approach. This approach encompasses geophysical methods, such as ERT, frequency electromagnetic conductivity, GPR, primary-wave refraction, multispectral analysis of shear-waves, natural gamma radiation, induction conductivity, and magnetic susceptibility [16]. In 2023, Wróbel conducted the interpretation of a landslide by integrating various geophysical methods, such as ERT, SRT, and Multi-channel Analysis of the Surface Waves (MASW) with remote sensing data analysis [17]. In 2019, Pupatenko employed a study to interpret the GPR data in dip survey cases [18]. In 2023, Zhang underscored the rapid and effective assessment of landslide-prone subsurface conditions. By employing the MASW and ERT techniques in tandem, the study provides valuable insights to evaluate landslide risks and proactively address the potential threats of debris flow [19]. In 2023, Hojat used the time-lapse ERT and Time-Domain Reflectometry (TDR) in order to monitor a rainfall-triggered landslide [20]. In 2022, Hussain proposed an amalgamation of the Emitted Seismic and ambient noise based geophysical methods. A review of applicable UAV-based methods in landslide study is also presented [21]. In 2022, Adella Syavira Studied the slip surface geometry of a landslide by leveraging the GPR data [22].

To identify the optimal resistivity distribution aligning with experimentally derived apparent resistivity values, inverse techniques become imperative. In geophysical exploration, forward modelling plays a crucial role, enabling the computation of model responses throughout the inversion procedure. Various established algorithms address the inversion of geoelectrical data, with some specifically tailored for monitoring (time-lapse) observations or integrating hydrological and other geophysical data into the inversion process [23]. The pyGIMLi framework [24] and ResIPy [23] represent successful instances of open-source programs, both functioning as Python Application Programming Interfaces (API). Notably, ResIPy stands out as an exemplar of a Graphical User Interface (GUI), enhancing user-friendliness by simplifying the utilization of intricate codes. While ResIPy focuses exclusively on the ERT and induced polarization modelling, the pyGIMLi presents a broader range of frameworks. It provides diverse seismic methods (i.e., refraction tomography modelling in 2D and 3D, cross-hole tomography, and etc.), magnetometry, gravimetry, and electromagnetic data processing, modelling, and inversion. In 2023, Rochlitz leveraged custEM open-source software in order to employ a forward modelling and utilized pyGIMLi to conduct a three-dimensional inversion on electromagnetic data [25]. In 2023, Steiner proposed a versatile library for the management of seismic refraction data, functioning on the foundation of pyGIMLi's Seismic Refraction Manager [26]. In 2015, Cockett introduced SimPEG, an open-source framework for simulation and gradient-based parameter estimation in geophysical applications [27]. In 2022, Guedes represented Refrapy, a Python program for seismic refraction data analysis [28].

The Seismic Refraction Tomography (SRT) has proven to be a valuable tool in the study of landslides, particularly in the characterization of sliding zone geometries [15]. However, employing this method for the long-term monitoring of landslides poses challenges, primarily attributable to potential errors stemming from topographic variations[3]. Despite these inherent challenges, the utilization of the SRT in landslide investigations has been widespread, marked by notable advancements in algorithm development and the establishment of robust field-data collection systems [5]. Notably, researchers have addressed the limitations of the SRT by integrating it with other geophysical methods, such as ERT. This integration has proven effective in delineating landslide body geometries and identifying critical sliding surfaces [15]. This collaborative approach enhances the comprehensiveness and accuracy of landslide studies, showcasing the adaptability and continued progress within the field despite the acknowledged challenges associated with long-term monitoring and topographic variations.

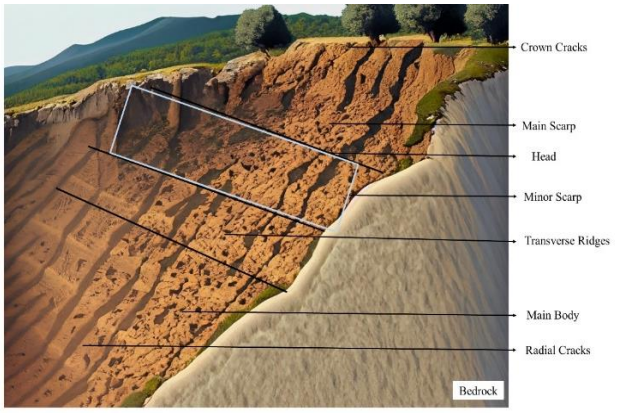

Fig.1 A simplified Schematic visualization of a landslide system.

In this study, both ERT and SRT simulations are employed for a synthetic landslide model through unstructured meshing, conducted by utilizing pyGIMLi library, version 1.4.3. The operating system utilized for the forward and inverse modelling is a laptop with 16GB RAM and a 12th Gen Intel® Core™ i7 1255U CPU.

2. Methodology

This study aims to explore a synthetic landslide comprising three layers through the integration of both ERT and SRT simulations. To achieve this, the forward modelling of aforementioned geophysical methods is employed firstly. In the context of geophysical simulations and modelling, it is common to do such modelling. In fact, the forward produced model act as an input in the inversion process. A mesh is generated, and forward simulations yield apparent resistivity data for diverse electrode configurations, emulating field acquisition. Simultaneously, the SRT simulations are performed. The synthetic model undergoes finite element-based discretization, and travel time data are generated for various source-receiver configurations. The accuracy of these simulations is evaluated through statistical metrics, such as resolution, sensitivity, and inversion misfit, providing insights into the methodology's robustness.

2.1. Forward modelling

In geophysics, the forward problem is a fundamental aspect involving the computation of responses under the assumption of known sources and earth models. This is expressed as:

$$F_j\,[m] = d_j^{obs} \equiv d_j + n_j \qquad j = 1, \dots, N \tag{1}$$

Here, $\boldsymbol{F_j}$ represents a forward modelling operator, incorporating intricate details of survey design and pertinent physical equations. The symbol $\boldsymbol{m}$ conventionally denotes the distribution of physical properties, while the right side portrays the observed datum $\boldsymbol{d_j^{obs}}$, comprising the true datum $\boldsymbol{d_j}$ and additive noise $\boldsymbol{n_j}$. The operator $\boldsymbol{F}$ manifests diversely, often adopting integral or differential forms, necessitating numerical solutions for resultant equations. Despite challenges, such as the computational demands for electromagnetic responses in a 3D Earth, the forward modelling quandary remains well-

posed, yielding a unique solution [29].

This understanding of the forward problem is integral to geophysical exploration and plays a key role in the development of inversion algorithms [30]. The process of inversion relies on resolving the forward problem, wherein data is computed from a specified set of model parameters. While inverse problems often presume a perfect knowledge of the forward problem solution, practical execution, encapsulated in the forward-modelling process, is inherently susceptible to errors, acknowledged as modelling errors [31].

Forward modelling, serving as a research and educational tool, is particularly crucial in applied geophysics. Geophysical approaches, such as gravimetry, magnetometry, and geoelectrical methods are employed to probe the Earth's subsurface. The presentation of forward models for these geophysical techniques, employing the finite-element method, is a significant contribution to advancing our understanding of the subsurface Earth processes [32].

2.2. Inverse modelling

Extensive research has been dedicated to the concept of inverse problems in geophysics, particularly in the field of employing diverse computational methods to tackle these challenges [33]. Within this context, a central key lies in crafting stable solutions capable of resolving intricate geological structures. This challenge has spurred the development of innovative techniques, including the introduction of focusing inversion images [34].

To address the intricacies of discrete inverse problems in geophysics, a conceptual framework has been proposed. This framework [35] underscores the significance of information and measurements in defining the calibration target and objective function. It emphasizes the need for a systematic approach to handle the complexities inherent in geophysical inverse problems. The evolution of inversion theory in geophysics has played a pivotal role in advancing the field. Notably, the focus has shifted towards introducing new criteria to navigate challenges arising from inaccurate and inconsistent data [36]. This progressive development in inversion theory contributes to refining the methodologies employed in geophysical studies, thereby enhancing the capacity to derive meaningful insights from complex and real-world geological scenarios.

A range of studies have explored the use of inversion techniques in the electrical resistivity tomography. In 2002, Tamburrino proposed a non-iterative inversion method based on the monotonicity of the resistance matrix and its numerical approximations [37]. In 2022, Fallah Safari proposed a smoothness constrained inversion algorithm for 2.5-dimensional forward modelling, which was found to provide stable and accurate results [38]. In 2022, Cozzolino applied the Extended data-adaptive Probability-based Electrical Resistivity Tomography Inversion Method (E-PERTI) to model the resistivity distribution of a large dataset, successfully identifying an ancient ditch [39]. In 2002, J. LaBrecque tested an anisotropic inversion algorithm, which produced images less prone to artifacts and noise, and was faster than older algorithms. These studies collectively demonstrate the potential of inversion techniques in enhancing the accuracy and efficiency of the electrical resistivity tomography [40].

The seismic refraction technique stands as a robust geophysical instrument widely utilized in engineering geology, geotechnical engineering, and exploration geophysics. To ensure trustworthy outcomes, precise processing of seismic refraction data, particularly in the inversion phase, is crucial [41]. A range of studies have explored the use of seismic refraction tomography in various geological settings. In 1985, Mooney developed a method for the direct inversion of seismic refraction data in planar dipping structures, successfully applying it to synthetic seismograms and field data [42]. In 1989, White presented an iterative tomographic inversion scheme for determining 2-D velocity structure from seismic refraction first-arrival travel times, with a focus on source/receiver spacing and resolution [43]. In 1988, Mora proposed an iterative inversion method that combines migration and reflection tomography, emphasizing the importance of a varying background velocity [44]. In 2003, Hobro extended this work to 3-D tomographic inversion of combined reflection and refraction seismic travel time data, demonstrating its application to real data in the Cascadia Margin. These studies collectively highlight the potential of seismic refraction tomography in characterizing subsurface structures [45]. In 2011, Alimoradi detailed an investigation into the utilization of neural networks for addressing geophysical inverse problems. Specifically, the study focuses on employing a three-layer feed-forward neural network for estimating the depth of dikes through magnetic data. The training process involves the use of synthetic data as both input and output, employing the back-propagation algorithm for the forward neural network training. In 2012 and 2013, Alimoradi employed feed-forward artificial neural networks (FNNs) and support vector regression machines (SVR) to establish a connection between identified synthetic attributes and synthetic porosity values within a specified environment [46], [47].

Inverse modelling without considering constraints for any geophysical data is inherently non-unique, primarily due to the likelihood of multiple geological models (e.g., resistivity, and V_P distributions) that are consistent with observed data. Consequently, it becomes necessary to impose constraints on the inversion model. Additionally, without appropriate constraints, errors (such as rounding errors in numerical values) can lead to an unstable solution.

In order to formulate the inverse problem in both ERT and SRT studies, the distribution of electrical and seismic properties is discretized into sets of parameters defining the model vector m. While for one-dimensional problems, in the case of ERT study, $\boldsymbol{m}$ typically includes the conductivity and thickness of a multi-layered model. In the SRT scenario, $\boldsymbol{m}$ includes the refracted waves' travel times and the geometric properties of the model. For arbitrary two-dimensional and three-dimensional distributions, its cells generally correspond to the conductivity and travel times of the individual finite elements (FEs) or finite difference (FD) components used in forward modelling. This implies that, for such cases, each cell aligns with the conductivity (in the ERT scenario) and wave travel times (in the SRT scenario) of the corresponding FE or FD element in the forward modelling process.

$$m_j = ln\sigma_j \qquad j = (1, \dots, M) \tag{2}$$

Here, the logarithm is employed to calculate the range of ground conductivity. Similarly, a given dataset of measured resistances, R_i, results in a data vector m according to Equation (3).

$$d_i = -lnR_i \qquad i = (1, \dots, N) \tag{3}$$

Again, the transformed data are typically utilized upon entering the system, often due to the wide range of observed resistances for arbitrary electrode arrays. Meanwhile, the negative sign in Equation (3) in one-dimensional physics corresponds to Equation (2).

Given the non-uniqueness of the inverse problem for resistivity and wave propagation, coupled with the presence of data errors, effective numerical solutions often necessitate additional constraints imposed on the inversion process. This is typically achieved by treating the inversion problem as a regularized optimization problem, where the objective function takes the form of Equation (4).

$$\varphi_{total} = \varphi_d + \alpha\varphi_m \tag{4}$$

In order to minimize Equation (4), we have:

$$\varphi_d = \big(d - F(m)\big)^T W_d^T W_d (d - F(m)) \tag{5}$$

where $\boldsymbol{d}$ represents the data (e.g., measured apparent resistivities and apparent velocities), $\boldsymbol{F(m)}$ is a set of forward model estimates corresponding to the parameter set $\boldsymbol{m}$, and $\boldsymbol{W_d}$ is a data weight matrix. If the case of unrelated measurement errors is considered and by also neglecting the model errors, $\boldsymbol{W_d}$ becomes a diagonal matrix with entries equal to the standard deviation of each measurement.

For a one-dimensional DC electrical sounding problem, $\boldsymbol{m}$ is obtained from sets of apparent resistivities and thicknesses of the relevant layers. In the case of a two-dimensional resistivity imaging problem, $\boldsymbol{m}$ comprises sets of apparent resistivities in a two-dimensional grid (or mesh). Likewise, in the case of a two-dimensional refraction seismic imaging, $\boldsymbol{m}$ includes apparent velocities of the refracted waves

between source and the receiver.

One can express an arbitrary level of data inconsistency, given the number of measurements. In the Occam solution, the objective is to minimize Equation (4), subject to the constraint of the maximum value of $\boldsymbol{a}$. While using the Gauss-Newton approach, this leads to the iterative solution of Equation (6), where $\boldsymbol{\alpha}$ is a scalar controlling the regularization.

$$(j^T W_d^T W_d J + \alpha R)\Delta m = j^T W_d^T (d - F(m_k)) - \alpha R m_k \quad (6) \tag{6}$$

$$m_{k+1} = m_k + \Delta m \tag{7}$$

$$j_{i,j} = \frac{\partial d_i}{\partial m_j} \tag{9}$$

The Jacobian matrix ($\boldsymbol{J}$), as computed by utilizing Equation (8), represents the sensitivity. $\boldsymbol{m_k}$ signifies the adjusted parameter, while k iterations take place, having a rate of $\Delta \boldsymbol{m}$ in parameter updating. In the context of DC resistivity inversion, it is customary to formulate the inverse problem by employing log-transformed apparent resistivities [38].

The Finite Element Method (FEM) relies on a variational formulation, integrating the differential equation across the model domain. This integration, represented as a summation of contributions from discrete finite elements, yields a system of algebraic equations approximating the solution. Notably, this system, of finite dimensions, diverges from the initial infinite-dimensional partial differential equations. This approach offers notable advantages in modelling intricate irregular regions, utilizing non-uniform meshes to precisely represent solution gradients, handling boundary conditions involving fluxes, and facilitating the development of high-order approximations. Furthermore, the assessment of discretization errors can be conducted cost-effectively, serving a dual purpose: validating computational accuracy and guiding an adaptive refinement process where meshes autonomously adjust to achieve solutions of desired accuracy optimally. Rooted in the FEM, the forward modelling approach is not only integral to geophysical exploration but also constitutes a foundational element in the evolution of inversion algorithms [48].

For the purpose of forward modelling, the FEM was employed. It is widely recognized that the modelling algorithms associated with the FEM are characterized by a slower computational pace, albeit offering enhanced precision when compared to the Finite Difference Method (FDM). The inherent challenge of FEM's slower computation is effectively mitigated through the utilization of unstructured meshes, enabling the method to achieve a balance between efficiency and precision in modelling [49]. In contrast, the conventional Finite Difference (FD) approach is known for its simplicity in construction and maintenance, relying on structured rectangular grids. However, this simplicity comes at the cost of limitations, as it precludes local grid refinement, and any alterations in grid size exert a considerable impact on the overall computational resources required. Recent decades have witnessed the evolution of the FE method to address such challenges, endowing it with the inherent capability to support unstructured meshes. This development proves particularly advantageous in the context of the direct current resistivity (DCR) approach, wherein modelling and inversion methods are tailored to leverage the flexibility offered by unstructured meshes [50].

In pyGIMLi, the inherent inversion framework relies on the generalized Gauss-Newton approach and is universally adaptable to diverse physical predicaments due to its compatibility with any provided forward operator. The inversion task is formulated as the minimization of an objective function, encompassing both data misfit and model constraints [24]. Throughout the iterative process, two primary parameters play a crucial role in governing the inversion procedure. The first of these parameters is chi-square ($\boldsymbol{\chi^2}$), which serves as a metric quantifying the disparity between the observed and predicted data. Chi-square provides a quantitative measure of the misfit within the inversion process and is calculated through Equation (9).

$$\chi^2 = \sum \frac{(O_i - E_i)^2}{E_i} \tag{9}$$

Where $\boldsymbol{O_i}$ is the observed frequency for the category $\boldsymbol{i}$ and $\boldsymbol{E_i}$ is the expected frequency for the category $\boldsymbol{i}$. It is worthy to mention that the sum is taken over all categories.

3. Numerical modelling of landslide

The synthetic landslide model consists of three layers with distinct geological properties (Fig.2c and Fig.3a). These layers, represented by polygons in a 2D space, include different kinds of rock and soil types. Table 1 details the properties of each sub-region, including the assumed material and the related physical properties (i.e., apparent resistivity and apparent velocity of refracted waves shown in Figs. 2a and 2b, respectively).

A network of electrodes is strategically positioned to capture the electrical resistivity distribution within the landslide model utilizing the Schlumberger array. This array is a common electrode array used in ERT studies. In this array, the current electrodes are usually fixed at the center, and potential electrodes are moved outward, creating different "spacing" or configurations [51]. A data scheme is then created containing the position of current and potential electrodes. As K is calculated by the mentioned positions, the aforementioned data scheme contains K as well. In ERT studies, the geometric factors (often denoted as K) represent the sensitivity of the measurement configuration to changes in subsurface resistivity. The geometric factor is influenced by the electrode positions and the specific array used for the ERT study. Different arrays have different sensitivities to subsurface structures [52]. In Fig. 4, each label (SL-1 to SL-7) represents a specific Schlumberger electrode spacing, and the plot is showing how the geometric factors (K) vary for each electrode configuration. These variations can be crucial in understanding the resolution and sensitivity of the ERT survey at different depths or for different subsurface features. The electrode positions are adapted to account for the slope of the terrain, ensuring an accurate representation of the subsurface resistivity. 25 electrodes have been assigned to the surface. As a result, the data scheme includes 112 data in total. The resistivity values for different geological regions are assigned based on the defined resistivity map. The resistivity distribution is visualized alongside electrodes on the ground surface (Fig.2a), and forward modelling is conducted to simulate the ERT data. It is worth mentioning that a plausible geological section is depicted in Fig.2c.

Also, in the case of SRT, the deployment of geophones, imperative for recording seismic data, is undertaken across the landslide model. Sensor positions are adjusted to accommodate the terrain slope, ensuring an accurate representation of subsurface properties. Additionally, it is pertinent to mention that a 24-channel seismometer is assumed, with a fixed inter-channel distance of 7 meters. The velocity distribution within the geological layers is assigned based on the predefined markers (Fig.2b).

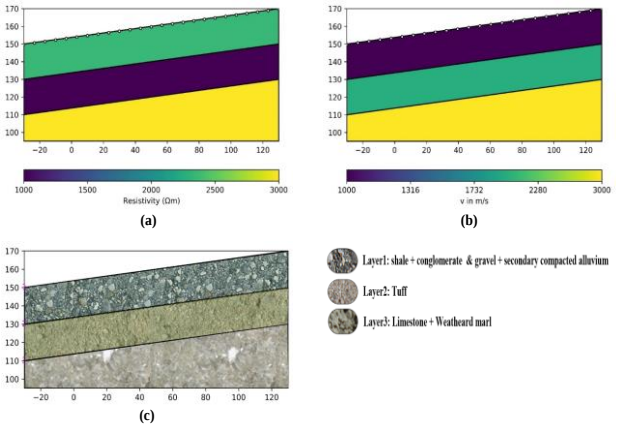

Fig. 2 A synthetic 2D landslide structure through simulating, (a) electrical resistivity model, (b) Vp model, and (c) a plausible geological section.

Table 1. The geophysical descriptions of the synthetic landslide model.

Layer	Resistivity (Ωm)	V_p (m/s)	Material
First layer	2350	1000	Shale+ Gravel+ Compacted Alluvium
Second layer	1000	2000	Tuff
Third layer	3000	3000	Limestone

The simulated ERT and SRT data are generated by incorporating resistivity and V_p values into the forward mesh (Fig.3a). Noise is introduced to mimic real-world conditions, and the data are processed to remove inconsistencies [53]. In this study, a value of 3% of the Gaussian noise is considered while simulating the data. Figure 4a illustrates the simulated ERT data. Also, Figure 5a shows the forward simulated refraction seismic data.

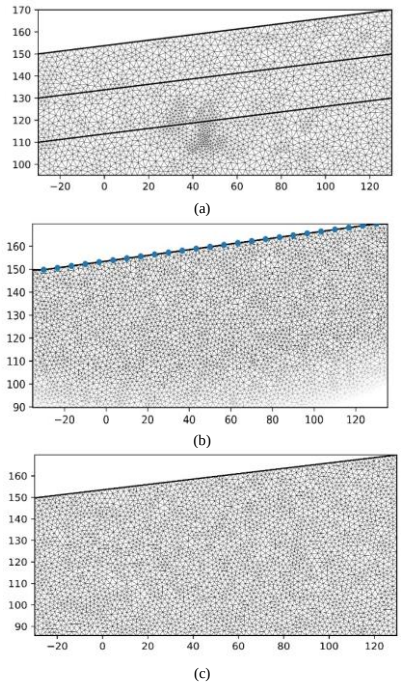

Fig. 3 The mesh quality of the synthetic landslide model for forward modelling (a), and inverse modelling of the ERT (b), and the SRT (c).

Following the completion of forward modelling, the generated model and simulated data for each scenario are introduced as inputs for the subsequent inverse modelling phase. As previously mentioned, the inversion process is conducted using the Simultaneous Iterative Reconstruction Technique (SIRT). Fig.4b illustrates the inversion response of the ERT data after two iterations, while Figure 5b presents the inversion response of the SRT simulated data after 10 iterations.

To assess the convergence and accuracy of the inversion process, Fig.4c and Fig.5c depict the misfit between the observed data and the inversion response for the ERT and SRT scenarios, respectively. These misfit figures provide valuable insights into the iterative refinement of the inversion results, highlighting the convergence of the SIRT and its effectiveness in minimizing the disparity between observed and predicted data.

The iterative inversion approach is further enhanced through the refinement of the inversion mesh in each iteration. Figures 3b and 3c visually represent the inverse mesh for both ERT and SRT scenarios, respectively, showcasing the evolving precision of the inversion process. After the culmination of iterations, the final inversion results are obtained and presented in Fig.6a for the ERT and Fig.6b for the SRT. These comprehensive figures incorporate the primary layers and superimpose ray paths, providing a consolidated visualization of the refined subsurface models. The inclusion of primary layers and ray paths in the final results contributes to a more interpretable and accurate representation of the subsurface characteristics, demonstrating the efficacy of the iterative inversion process in achieving a refined and reliable outcome.

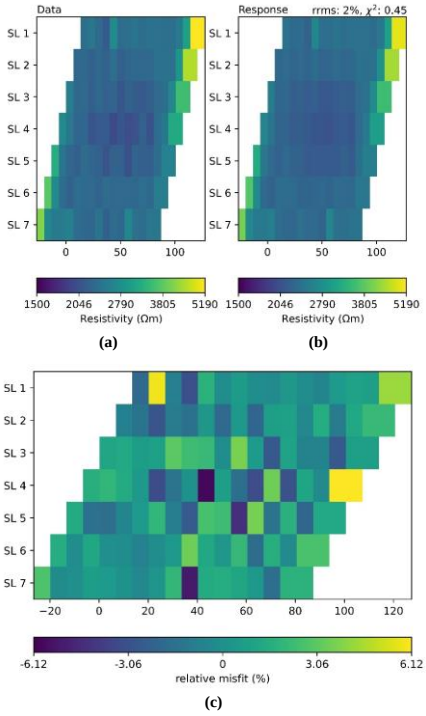

Fig. 4 The electrical resistivity data visualization, (a) observed apparent resistivity, (b) predicted apparent resistivity, and (c) misfit data.

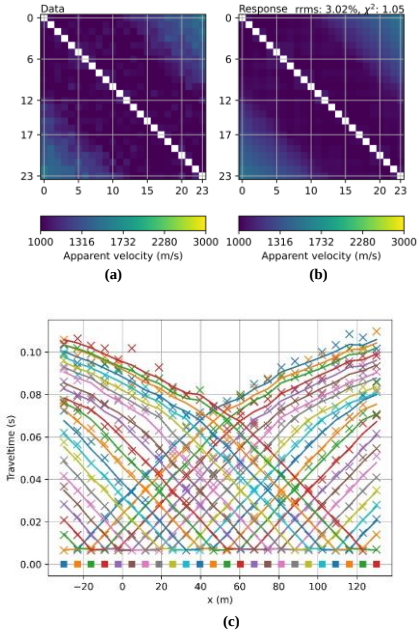

Fig. 5 The refraction seismic data visualization, (a) observed apparent velocity, (b) predicted apparent velocity, and (c) observed and predicted first arrival times (cross symbol shows predicted data).

4. Discussion

This study delves into the intricate analysis of landslides through the adept utilization of both Electrical Resistivity and Seismic Refraction Tomography simulations, with a strong emphasis on leveraging the capabilities of the pyGIMLi framework. In scrutinizing the heterogeneity of the media, the findings of this study showcase a notable correlation between the ERT and SRT inversion results. The ERT inversion reveals that the first layer exhibits the least heterogenous properties, a characteristic later confirmed by the SRT inversion. The dense coverage of ray paths in the first layer, as depicted in Fig. 6b, aligns seamlessly with the ERT interpretation. This synchronization underscores the efficacy of integrating geophysical methods, the ERT and SRT in particular, in offering a cohesive analysis of media heterogeneity across different geophysical techniques.

Fig. 6 collectively provides a compelling insight into bedrock detection. The ERT inversion highlights higher electrical resistivity in the third layer, potentially indicative of bedrock features, such as limestone. The SRT model complements this observation, as the ray paths deliberately avoid penetrating the third layer, a characteristic consistent with bedrock identification. The synergy between ERT and SRT strengthens the reliability of the bedrock detection assessments.

The exclusive derivation of moisture content obtained from the ERT proves pivotal in our study. Low resistivity values in the ERT results suggest areas with potentially higher moisture content. Th understanding of moisture dynamics is crucial for a comprehensive analysis of landslide-prone areas.

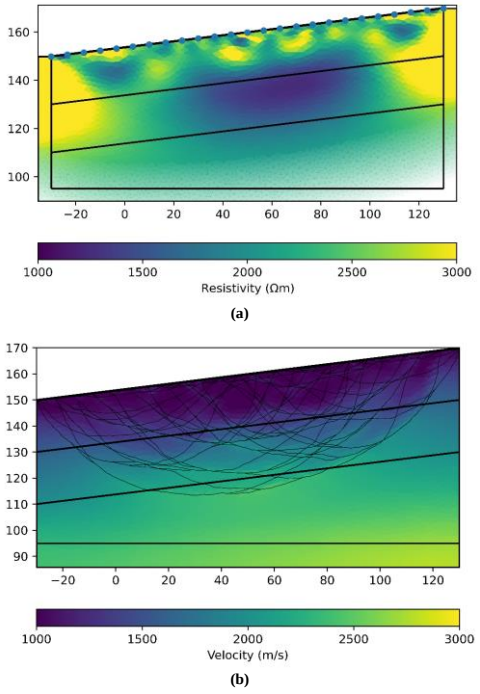

Fig. 6 The inversion result for (a) electrical resistivity, and (b) Vp. The boundary of assumed layers has been superimposed on the models.

5. Conclusion

The outcomes derived from this investigation showcase the effectiveness of integrating both Electrical Resistivity Tomography (ERT) and Seismic Refraction Tomography (SRT) for a comprehensive understanding of landslide characteristics. The synergistic correlation between these methodologies fortifies the robustness of our conclusions. Notably, in Fig. 6, the visual representation further substantiates the credibility of the interpretation, elucidating intricate subsurface conditions. The achievement of this study underscores the proficiency of the proposed framework in handling diverse geophysical data, thereby facilitating a holistic interpretation of landslide parameters. It is pertinent to introduce intelligent algorithms as a contemporary alternative for inversion methodologies. Integrating such algorithms can augment the efficiency and adaptability of the proposed framework. The success of this study, as highlighted, emphasizes the intricate insights into media heterogeneity, bedrock detection, and moisture content, all of which hold significant implications for the landslide risk assessment. Therefore, in addition to the synergy between the ERT and SRT approaches, it is recommended to explore intelligent algorithms in future research endeavors. This inclusion aligns with the evolving landscape of inversion techniques and positions the study at the forefront of incorporating cutting-edge methodologies for improved subsurface property studies and informed risk mitigation strategies.

Acknowledgements

Special thanks to the School of Mining Engineering for providing a conducive academic environment. I am grateful to Miss Kiana Damavandi for her exceptional support and contributions to this research. Appreciation to everyone who played a role in this endeavor, contributing to its success.

REFERENCES

[1] S. Morelli, S. Utili, V. Pazzi, R. Castellanza, and X. Fan, 'Landslides and Geophysical Investigations: Advantages and Limitations', International Journal of Geophysics, vol. 2019. Hindawi Limited, 2019. doi: 10.1155/2019/8732830.

[2] D. Jongmans and S. Garambois, 'Geophysical investigation of landslides: a review', vol. 178, no. 2, pp. 101–112, 2007, doi: 10.2113/gssgfbull.178.2.101ï.

[3] J. S. Whiteley et al., 'Landslide monitoring using seismic refraction tomography – The importance of incorporating topographic variations', Eng Geol, vol. 268, p. 105525, Apr. 2020, doi: 10.1016/J.ENGGEO.2020.105525.

[4] S. Carpentier, M. Konz, R. Fischer, G. Anagnostopoulos, K. Meusburger, and K. Schoeck, 'Geophysical imaging of shallow subsurface topography and its implication for shallow landslide susceptibility in the Urseren Valley, Switzerland', J Appl Geophy, vol. 83, pp. 46–56, Aug. 2012, doi: 10.1016/J.JAPPGEO.2012.05.001.

[5] P. Imani, A. Abd El-Raouf, and G. Tian, 'Landslide investigation using seismic refraction tomography method: A review', Annals of Geophysics, vol. 64, May 2021, doi: 10.4401/AG-8633.

[6] G. Pappalardo, S. Imposa, M. S. Barbano, S. Grassi, and S. Mineo, 'Study of landslides at the archaeological site of Abakainon necropolis (NE Sicily) by geomorphological and geophysical investigations', Landslides, vol. 15, no. 7, pp. 1279–1297, Jul. 2018, doi: 10.1007/s10346-018-0951-y.

[7] J. S. Whiteley et al., 'Rapid characterisation of landslide heterogeneity using unsupervised classification of electrical resistivity and seismic refraction surveys', Eng Geol, vol. 290, Sep. 2021, doi: 10.1016/j.enggeo.2021.106189.

[8] S. Rezaei, I. Shooshpasha, and H. Rezaei, 'Reconstruction of landslide model from ERT, geotechnical, and field data, Nargeschal landslide, Iran', Bulletin of Engineering Geology and the Environment, vol. 78, no. 5, pp. 3223–3237, Jul. 2019, doi: 10.1007/s10064-018-1352-0.

[9] M. Zainal, B. Munir, M. Yanis, and A. Muhni, 'Characterization

of Landslide geometry using Seismic Refraction Tomography in the GayoLues, Indonesia', 2021. [Online]. Available: https://ejournal2.undip.ac.id/index.php/jpa/index

[10] Q. U. Rehman, W. Ahmed, M. Waseem, S. Khan, A. Farid, and S. H. A. Shah, 'Geophysical investigations of a potential landslide area in mayoon, hunza district, gilgit-baltistan, pakistan', Rudarsko Geolosko Naftni Zbornik, vol. 36, no. 3, pp. 127–141, 2021, doi: 10.17794/rgn.2021.3.9.

[11] J. Yang et al., 'Seismic Characterization of a Landslide Complex: A Case History from Majes, Peru', Sustainability (Switzerland), vol. 15, no. 18, Sep. 2023, doi: 10.3390/su151813574.

[12] K. Damavandi, M. Abedi, G. H. Norouzi, and M. Mojarab, 'Geoelectrical modelling of a landslide surface through an unstructured mesh', Bulletin of Geophysics and Oceanography, vol. 63, no. 2, pp. 337–356, Jun. 2022, doi: 10.4430/bgo00384.

[13] Q. Chen, S. Zhang, S. Chang, B. Liu, J. Liu, and J. Long, 'Geophysical Interpretation of a Subsurface Landslide in the Southern Qinshui Basin', J Environ Eng Geophys, vol. 24, no. 3, pp. 433–449, Sep. 2019, doi: 10.2113/JEEG24.3.433.

[14] B. Pasierb, M. Grodecki, and R. Gwóźdź, 'Geophysical and geotechnical approach to a landslide stability assessment: a case study', Acta Geophysica, vol. 67, no. 6, pp. 1823–1834, Dec. 2019, doi: 10.1007/s11600-019-00338-7.

[15] M. Himi et al., 'Application of Resistivity and Seismic Refraction Tomography for Landslide Stability Assessment in Vallcebre, Spanish Pyrenees', Remote Sens (Basel), vol. 14, no. 24, Dec. 2022, doi: 10.3390/rs14246333.

[16] D. Huntley, P. Bobrowsky, M. Hendry, R. Macciotta, and M. Best, 'Multi-technique Geophysical Investigation of a Very Slow-moving Landslide near Ashcroft, British Columbia, Canada', J Environ Eng Geophys, vol. 24, no. 1, pp. 87–110, Mar. 2019, doi: 10.2113/JEEG24.1.87.

[17] M. Wróbel et al., 'Integrated Geophysical Imaging and Remote Sensing for Enhancing Geological Interpretation of Landslides with Uncertainty Estimation—A Case Study from Cisiec, Poland', Remote Sens (Basel), vol. 15, no. 1, Jan. 2023, doi: 10.3390/rs15010238.

[18] V. Pupatenko, Y. Sukhobok, G. Stoyanovich, A. Stetsyuk, and L. Verkhovtsev, 'GPR data interpretation in the landslides and subgrade slope surveys', MATEC Web of Conferences, vol. 265, p. 03003, 2019, doi: 10.1051/matecconf/201926503003.

[19] G. Zhang, F. Tu, Y. Tang, X. Chen, K. Xie, and S. Dai, 'Application of geophysical prospecting methods ERT and MASW in the landslide of Daofu County, China', Front Earth Sci (Lausanne), vol. 10, Jan. 2023, doi: 10.3389/feart.2022.1054394.

[20] A. Hojat et al., 'Geoelectrical characterization and monitoring of slopes on a rainfall-triggered landslide simulator', J Appl Geophy, vol. 170, Nov. 2019, doi: 10.1016/j.jappgeo.2019.103844.

[21] Y. Hussain et al., 'Review on the Geophysical and UAV-Based Methods Applied to Landslides', Remote Sensing, vol. 14, no. 18. MDPI, Sep. 01, 2022. doi: 10.3390/rs14184564.

[22] Adella Syavira, Y Yatini, and Wrego Seno Giamboro, 'Identification of landslide potential based on Ground Penetrating Radar (GPR) data in Prambanan District, Sleman, Yogyakarta', Global Journal of Engineering and Technology Advances, vol. 13, no. 2, pp. 071–078, Nov. 2022, doi: 10.30574/gjeta.2022.13.2.0193.

[23] G. Blanchy, S. Saneiyan, J. Boyd, P. McLachlan, and A. Binley, 'ResIPy, an intuitive open source software for complex geoelectrical inversion/modeling', Comput Geosci, vol. 137, p. 104423, Apr. 2020, doi: 10.1016/J.CAGEO.2020.104423.

[24] C. Rücker, T. Günther, and F. M. Wagner, 'pyGIMLi: An open-source library for modelling and inversion in geophysics', Comput Geosci, vol. 109, pp. 106–123, Dec. 2017, doi: 10.1016/j.cageo.2017.07.011.

[25] R. Rochlitz, M. Becken, and T. Günther, 'Three-dimensional inversion of semi-airborne electromagnetic data with a second-order finite-element forward solver', Geophys J Int, vol. 234, no. 1, pp. 528–545, Jul. 2023, doi: 10.1093/gji/ggad056.

[26] M. Steiner and A. Flores Orozco, 'formikoj: A flexible library for data management and processing in geophysics—Application for seismic refraction data', Comput Geosci, vol. 176, p. 105339, Jul. 2023, doi: 10.1016/J.CAGEO.2023.105339.

[27] R. Cockett, S. Kang, L. J. Heagy, A. Pidlisecky, and D. W. Oldenburg, 'SimPEG: An open source framework for simulation and gradient based parameter estimation in geophysical applications', Comput Geosci, vol. 85, pp. 142–154, Dec. 2015, doi: 10.1016/J.CAGEO.2015.09.015.

[28] V. J. C. B. Guedes, S. T. R. Maciel, and M. P. Rocha, 'Refrapy: A Python program for seismic refraction data analysis', Comput Geosci, vol. 159, Feb. 2022, doi: 10.1016/j.cageo.2021.105020.

[29] Douglas W. Oldenburg and Yaoguo Li, 'Fundamentals of Inversion Near-Surface Geophysics Part 1: Concepts and Fundamentals', 2005. [Online]. Available: http://library.seg.org/

[30] T. Chen and G. Zhang, 'Forward modeling of gravity anomalies based on cell mergence and parallel computing', Comput Geosci, vol. 120, pp. 1–9, Nov. 2018, doi: 10.1016/j.cageo.2018.07.007.

[31] T. M. Hansen, K. S. Cordua, B. H. Jacobsen, and K. Mosegaard, 'Accounting for imperfect forward modeling in geophysical inverse problems - Exemplified for crosshole tomography', Geophysics, vol. 79, no. 3, pp. H1–H21, Mar. 2014, doi: 10.1190/GEO2013-0215.1.

[32] S. L. Butler and G. Sinha, 'Forward modeling of applied geophysics methods using Comsol and comparison with analytical and laboratory analog models', Comput Geosci, vol. 42, pp. 168–176, May 2012, doi: 10.1016/j.cageo.2011.08.022.

[33] V. Pereyra, H. B. Keller, and W. H. K. Lee, 'COMPUTATIONAL METHODS FOR INVERSE PROBLEMS IN GEOPHYSICS: INVERSION OF TRAVEL TIME OBSERVATIONS', 1980.

[34] O. Portniaguine and M. S. Zhdanov, 'Focusing geophysical inversion images', 1999. [Online]. Available: http://library.seg.org/

[35] M. Giudici et al., 'A conceptual framework for discrete inverse problems in geophysics', Jan. 2019, [Online]. Available: http://arxiv.org/abs/1901.07937

[36] Mitsuhiro MATSU'URA, 'Development of Inversion Theory in Geophysics', 1991.

[37] A. Tamburrino and G. Rubinacci, 'A new non-iterative inversion method for electrical resistance tomography', Inverse Probl, vol. 18, no. 6, pp. 1809–1829, Dec. 2002, doi: 10.1088/0266-5611/18/6/323.

[38] M. Fallah Safari and R. Ghanati, 'DC Electrical Resistance Tomography Inversion', Journal of the Earth and Space Physics, vol. 47, no. 4, pp. 87–98, Dec. 2022, doi: 10.22059/JESPHYS.2021.323911.1007321.

[39] M. Cozzolino, P. Mauriello, and D. Patella, 'The Extended Data-Adaptive Probability-Based Electrical Resistivity Tomography

Inversion Method (E-PERTI) for the Characterization of the Buried Ditch of the Ancient Egnazia (Puglia, Italy)', Applied Sciences (Switzerland), vol. 12, no. 5, Mar. 2022, doi: 10.3390/app12052690.

[40] D. J. LaBrecque and D. Casale, 'Experience With Anisotropic Inversion For Electrical Resistivity Tomography', in 15th EEGS Symposium on the Application of Geophysics to Engineering and Environmental Problems, European Association of Geoscientists & Engineers, Feb. 2002, p. cp-191-00010. doi: 10.3997/2214-4609-pdb.191.11ELE6.

[41] R. Poormirzaee, R. H. Moghadam, and A. Zarean, 'Inversion seismic refraction data using particle swarm optimization: a case study of Tabriz, Iran', Arabian Journal of Geosciences, vol. 8, no. 8, pp. 5981–5989, Aug. 2015, doi: 10.1007/s12517-014-1662-x.

[42] D. Mooney and W. M. Kohler, 'Inversion of seismic refraction data in planar dipping structure', 1985. [Online]. Available: https://academic.oup.com/gji/article/82/1/81/551363

[43] D. J. White, ' Two - Dimensional Seismic Refraction Tomography', Geophys J Int, vol. 97, no. 2, pp. 223–245, 1989, doi: 10.1111/j.1365-246X.1989.tb00498.x.

[44] P. Mora, 'Inversion-migration-t-tomography', 1988.

[45] J. W. D. Hobro, S. C. Singh, and T. A. Minshull, 'Three-dimensional tomographic inversion of combined reflection and refraction seismic traveltime data', 2003.

[46] A. Alimoradi and A. Moradzadeh, 'Reservoir Porosity Determination from 3D Seismic Data-Application of Two Machine Learning Techniques', 2012. [Online]. Available: https://www.researchgate.net/publication/258871568

[47] A. Alimoradi, A. Moradzadeh, and M. R. Bakhtiari, 'Application of Artificial Neural Networks and Support Vector Machines for carbonate pores size estimation from 3D seismic data', 2013.

[48] M. S. Jeshvaghani and M. Darijani, 'Two-dimensional geomagnetic forward modeling using adaptive finite element method and investigation of the topographic effect', *J Appl Geophy*, vol. 105, pp. 169–179, 2014, doi: 10.1016/j.jappgeo.2014.03.016.

[49] A. Binley, 'Tools and Techniques: Electrical Methods', *Treatise on Geophysics: Second Edition*, vol. 11, pp. 233–259, Jan. 2015, doi: 10.1016/B978-0-444-53802-4.00192-5.

[50] K. Damavandi, M. Abedi, G. H. Norouzi, and M. Mojarab, 'Geoelectrical modelling of a landslide surface through an unstructured mesh', *Bulletin of Geophysics and Oceanography*, vol. 63, no. 2, pp. 337–356, Jun. 2022, doi: 10.4430/bgo00384.

[51] J. Milsom and A. Eriksen, 'Field Geophysics, Fourth Edition', *Environmental & Engineering Geoscience*, vol. 19, no. 2, pp. 205–206, May 2013, doi: 10.2113/gseegeosci.19.2.205.

[52] T. Günther, C. Rücker, and K. Spitzer, 'Three-dimensional modelling and inversion of dc resistivity data incorporating topography - II. Inversion', *Geophys J Int*, vol. 166, no. 2, pp. 506–517, Aug. 2006, doi: 10.1111/j.1365-246X.2006.03011.x.

[53] V. der, G. Klaus Spitzer, B. Freiberg aD Peter Weidelt, and T. A. Braunschweig Maxwell Meju, 'Inversion Methods and Resolution Analysis for the 2D/3D Reconstruction of Resistivity Structures from DC Measurements', 2004.